

BI-DIRECTIONAL DC-AC CONVERTERS WITH HIGH FREQUENCY ISOLATION

R. L. Cardoso, I. Barbi

Instituto de Eletronica de Potencia, UFSC. Florianopolis - SC - Brasil

Emails: (robsonn, ivobarbi)@inep.ufsc.br

Abstract—For applications such as UPSs (uninterruptible power supplies) and new energy systems, e.g photovoltaic or fuel cell systems, it is essential to isolate the load or the photovoltaic cells from the grid. For these applications, the use of a converter that has high frequency isolation and also provides sinusoidal voltage would be very advantageous, since it would eliminate the low frequency transformer with an iron alloy core which is voluminous and and heavy besides frequently producing audible noise.

Index Terms - inverter, sepic, single-stage, bi-directional, DC-AC, UPS.

I. INTRODUCTION

For applications such as UPSs (uninterruptible power supplies) and new energy systems, e.g photovoltaic or fuel cell systems, it is essential to isolate the load or the photovoltaic cells from the grid for the following reasons: a) to prevent a DC current from flowing to the AC side; b) to prevent high fault currents from flowing through the converter; c) to protect the user against electrical shocks or leakage currents [1], and d) the need to adapt voltage level between battery and grid or battery and load. For these applications, the use of a converter that has high frequency isolation and also provides sinusoidal voltage would be very advantageous, since it would eliminate the low frequency transformer with an iron alloy core which is voluminous and and heavy besides frequently producing audible noise.

Currently, the solution most widely accepted and studied in literature are the matrix converters, shown in Fig. 1. These converters provide high frequency isolation by means of an inverter that produces symmetrical alternate voltage at high frequency which is applied to the primary terminals of the transformer, as shown in the Fig. 1(a), guaranteeing insulation [2]-[6]. The high frequency inverters used at primary can be the full-bridge, half-bridge, and push-pull types. In Fig. 1(c) and 1(d) some topologies are shown as examples. On the secondary side, instead of using a rectifier, as in the DC-DC converters, there is a modulator synchronized

with the inverter on the primary side whose function is to produce a sinusoidal PWM (SPWM) voltage which passes through an LC filter to eliminate the high frequency components, therefore, obtaining a sinusoidal voltage with an low high frequency ripple at the output. These converters present some inconveniences, such as the use of four quadrants switches, whose clamping and switching techniques are not fully established, beside problems related to transformer saturation.

In opposition to these direct DC-AC converters, in 1990 a flyback converter operating in four quadrants was presented in [7]-[8]. This converter was composed of two flybacks converters, as show in Fig. 2(c), with a differential connection at the output, as show in the block diagram of Fig. 2(a).

The bibliographical research in the specialized literature did not uncover another bi-directional converter with high frequency isolation using the output differential connection principle. This work aims to fill this void by proposing three more DC-AC isolated bi-directional converters based on the Cuk, sepic and zeta converters shown in Fig. 2(d), (e) and (f). In the sequence of this paper, the theoretical analysis and experimental results of a laboratory prototype of DC-AC bi-directional sepic with high frequency isolation will be presented.

II. THEORETICAL ANALYSIS FOR SEPIC DC-AC CONVERTER

A. Analysis of the main variable of the DC-AC bi-directional sepic converter with high frequency isolation

With the goal of obtaining a precise mathematical representation of DC-AC bi-directional sepic converter with high frequency isolation, shown in Fig. 3, from deduced equations, curves were drawn representing the most important variables of the converter.

The converter operates with the duty cycle $d(t)$ being applied to the switches S_1 and S_4 while the complementary duty cycle $d(t)'$ is applied to the switches S_2 and S_3 , as shown in Figs 4 and 5. The voltage across the

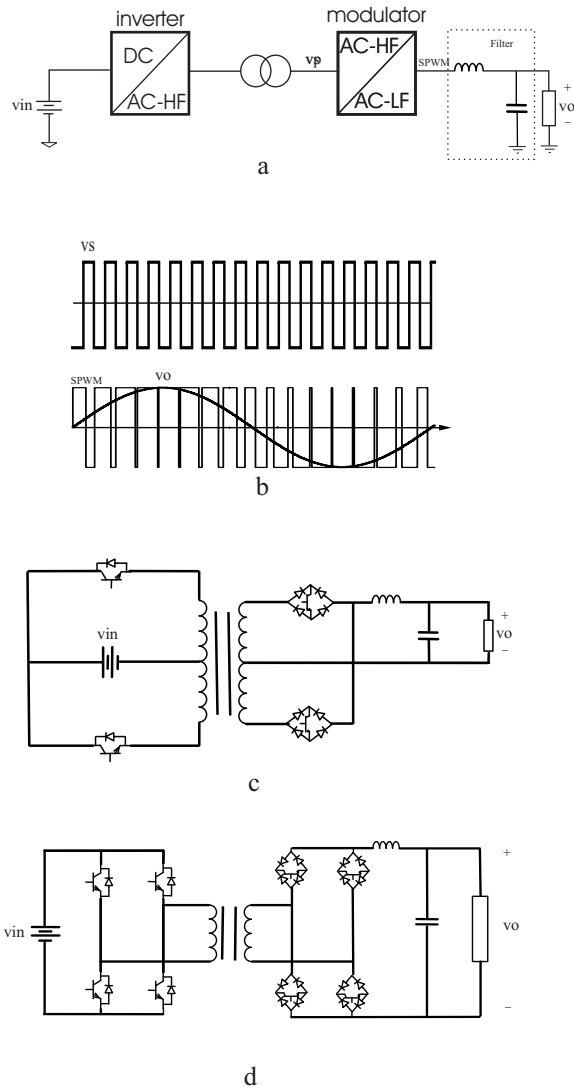


Fig. 1. Classic solution: a) Block diagram of the matrix converters b) Waveforms c) Push-pull matrix converter and d) Full-bridge matrix converter.

capacitors, $v_{C1}(t)$ and $v_{C2}(t)$, expressed by equations (1) and (2), represent the output voltage of each DC-DC converter, as shown in Fig 2(b), as a function of the duty cycle, which varies sinusoidally.

$$v_{C1}(t) = \frac{d(t)}{1-d(t)} V_{in} \quad (1)$$

$$v_{C2}(t) = \frac{1-d(t)}{d(t)} V_{in} \quad (2)$$

Subtracting voltage $v_{C2}(t)$ from voltage $v_{C1}(t)$ eliminates the average value of the output voltage, therefore, producing a purely sine voltage $v_o(t)$, represented for

the expression (3) and shown in the Fig. 2(b).

$$v_o(t) = v_{C1}(t) - v_{C2}(t) \quad (3)$$

In order to simplify the mathematics involved, the control will be analyzed considering that the converter operates with a resistive load. The voltage gain as a function of the duty cycle of converter is expressed by equation (4), where the input voltage was considered constant, i.e. V_{in} .

$$m(t) = \frac{v_o(t)}{V_{in}} = \frac{d(t)}{1-d(t)} - \frac{1-d(t)}{d(t)} = \frac{2d(t)-1}{d(t)(1-d(t))} \quad (4)$$

Where,

$$d(t) = 0.5 + \frac{V_{op}}{8nV_{in}} \sin(\omega t) \quad (5)$$

The output voltage, $v_o(t)$, as a function of the duty cycle is represented by the equation (6).

$$v_o(t) = (8d(t) - 4)V_{in} \quad (6)$$

B. Average Model of the Sepic DC-AC converter

Sepic converter, shown in Fig. 3, have two states, as shown in the Figs. 4 and 5.

Solving a group of state-space equations provided the open loop transfer function of the converter in the frequency domain, given by expression (7).

$$\frac{\hat{v}_o(s)}{\hat{d}(s)} = \frac{8V_{in}}{s^2(2LC) + s\left(\frac{4L}{R} + r_L C\right) + \frac{2r_L}{R} + 1} \quad (7)$$

Where,

\hat{d} is the variation of the duty cycle;

\hat{v}_o is the variation of the output voltage of the converter;

r_L is the resistance of the inductor L ;

V_{in} is input voltage;

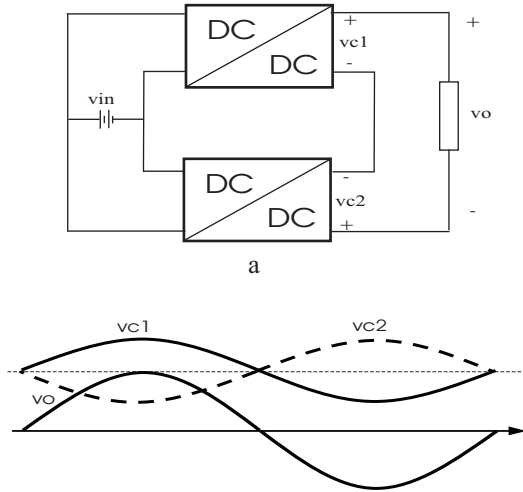
R is the load resistance;

C is the capacitance and

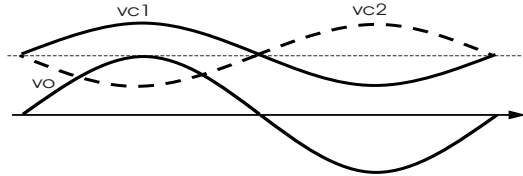
L is the inductance.

III. EXPERIMENTAL RESULTS

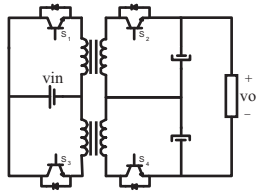
In order to validate the theoretical analysis and the simulations, a prototype, with the data shown in Table I, was implemented. The switches were implemented using IGBTs with inverse ultrafast diodes.



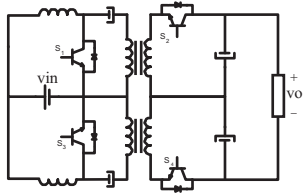
a



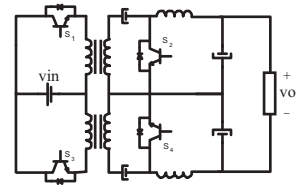
b



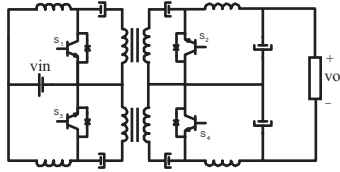
c



d



e



f

Fig. 2. Proposed converts: a)Block diagram b)Waveforms c)Based on the flyback converter d)Based on the sepic converter e)Based on the zeta converter and f)Based on the Cuk converter.

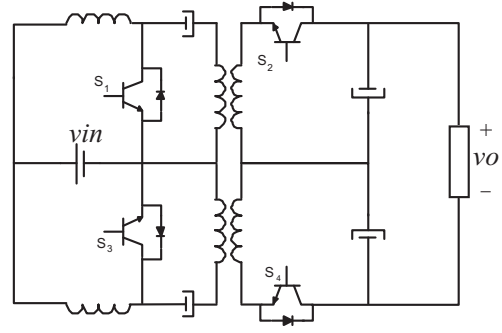


Fig. 3. New Bi-directional DC-AC Converter Sepic.

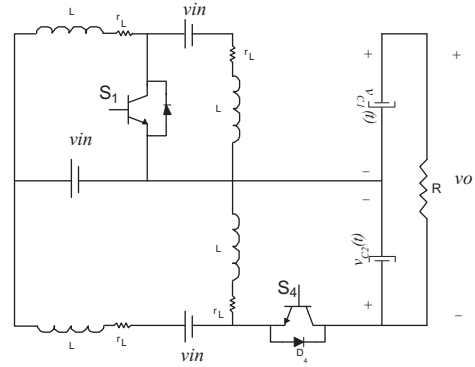


Fig. 4. Topologic state for $0 \leq D \leq DT$, S_1 and S_4 ON.

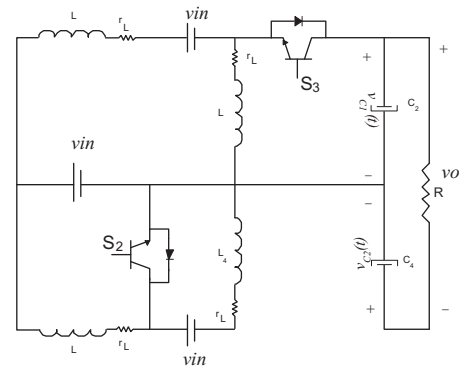


Fig. 5. Topologic state for $DT \leq D \leq T$, S_2 and S_3 ON.

TABLE I
DATA OF THE LABORATORY PROTOTYPE

Data of the laboratory prototype			
Input voltage V_{in}	100V	Induct. L	240 μ H
RMS out. volt. V_{orms}	115V	Capac. C	6,6 μ F
Out. freq. f_o	60Hz	IGBT $S_{1..4}$	IRG4PF50W
Out. power P_o	700VA	Diode D	MUR1560
Switching freq. f_s	65kHz		

Figure 6 shows the output voltage and the current (shown inverted for better visualization) of the converter operating in closed loop and with a resistive load. The output voltage has an RMS value of 115V and a frequency equal to 60Hz. The total harmonic distortion (THD) obtained was 4,89% using closed loop control.

The results, using closed loop control, for a 50% to 100% load variation are shown in the Fig. 7. The output voltage suffered a small disturbance which was promptly restored thanks to the designed controller, proving all the theoretical analysis and the simulation results. The total power efficiency can be improved to be 82.6%.

The output voltage and the current for motor induction load are shown in Fig. 8.

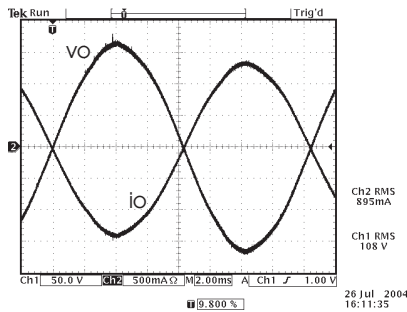


Fig. 6. Output voltage (v_o) and current (i_o) with resistive load.

IV. CONCLUSION

This paper presented an alternative to the DC-AC matrix converters which are the most widely studied solution in literature. Of the three new converters proposed, the DC-AC bi-directional sepic converter with high frequency isolation was chosen to be studied, projected and implemented. The laboratory prototype was used to obtain the experimental results presented here. This study concludes that the proposed converters are a feasible alternative to the existing solutions.

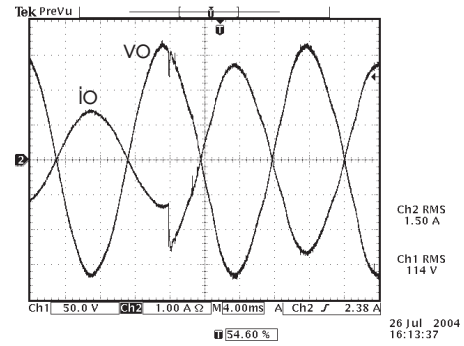


Fig. 7. Applying a load disturbance.

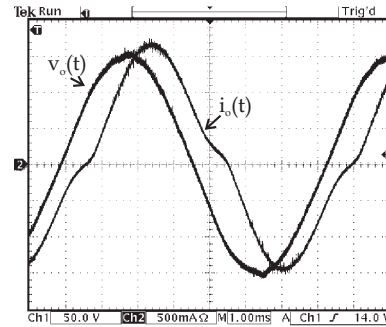


Fig. 8. Output voltage (v_o) and current (i_o) with induction motor.

ACKNOWLEDGMENT

The authors would like to thank the CNPQ.

REFERENCES

- [1] M. Matsui, and M. Yamagami, *Asymmetric control of HF link soft switching converter for UPS and PV systems with bidirectional power flow*, in Proc. IAS, pp. 1332-1340., Oct. 1998.
- [2] W. McMurray, *Power converter circuits having a high frequency link*, in U.S. Patent 3 517 300, June 1970.
- [3] S. Manias, and P. D. Ziogas, *A novel sinewave in ac to dc converter with high-frequency transformer isolation*, IEEE Trans. Ind. Electron, vol. IE-32, no. 4, pp. 430-438, Nov. 1985.
- [4] H. Harada, H. Sakamoto, and M. Shoyama, *Phase-controlled DC-AC converter with high-frequency switching*, IEEE Trans. Power Electron., vol. 3, pp. 406-411., Oct. 1988.
- [5] I. Yomato, N. Tokunaga, Y. Matsuda, H. Amano, and Y. Suzuki, *New conversion system for UPS using high frequency link*, in Proc. IEEE PESC88 Conf., pp. 658-663.
- [6] M. Koyama, K. Sanada, N. Sashida, and T. Kawabata, *High frequency link dclac converter with PWM cycloconverter for UPS*, Proc. of IPEC90 Conf., pp. 748-754..
- [7] G. Cimador, P. Prestifilippo, *An attractive new converter topology for AC/DC, DC/DC and DC/AC*, Proc. of INTELEC90 Conf., pp. 597-604.
- [8] G. Cimador, P. Prestifilippo, *A new generation of PWM ringing generators for telecommunications*, Proc. of INTELEC92 Conf., pp. 147-152.